URSI GASS 2021, Rome, Italy, 28 August - 4 September 2021

A Novel Detector for SETI on Radio Telescope Arrays

Kenneth M. Houston
Department of Astronomy, University of California Berkeley, Berkeley CA 94720

Abstract

The advent of SETI detection processing on interferometric telescopes presents challenges for signal processing. Beamforming the outputs of many dishes or aperture arrays is particularly difficult, requiring a very large number of beams to fill the primary field of view (FOV). Meanwhile the array gain is limited because of array sparseness. Incoherent beamforming (IBF) is the conventional alternative. IBF covers the primary FOV at a relatively low computational cost but has limited sensitivity. In this paper, an alternative to beamforming based on the observed covariance matrix is proposed. A method called Covariance Off-Diagonal Sum (CODS) computes the root-mean-square of the covariance matrix elements above the main diagonal, and is found to offer 3 dB (2x) improved sensitivity over IBF while still covering the primary FOV. The computational cost is approximately $N_{AP}/2$ times that of IBF, where N_{AP} is the number of apertures (dishes or aperture array stations), but could be orders of magnitude below beamforming over the full FOV. An Eigenvalue detector is also considered. We hypothesize that CODS will be less sensitive to RFI compared to IBF. The utility of CODS is not limited to narrowband signals in SETI, but could be useful for rapid detection of pulsars and fast radio bursts as well.

1 Introduction

Up to now, Radio SETI (Search for Extraterrestrial Intelligence) has been largely performed on single-dish radio telescopes. In the near future, multi-dish interferometric radio telescopes will be used for SETI. This will greatly improve sensitivity, but at the same time will increase computation and require new signal processing architectures. Combining signals from all the sensors can be particularly challenging. Because of large baselines, conventional beamforming produces very narrow beams, and may potentially require thousands of them to cover the primary field of view. For full FOV coverage, the number of beams is given by $N_{beam} = (D_{array}/D_{dish})^2$. As an example, the MeerKAT radio telescope in South Africa has 64 dishes of 13.5 meter diameter. Using all dishes with an 8 km array diameter, $(8000/13.5)^2 \approx 350,000$ beams are required! Even just using the array core, the numbers are large: for 44 dishes, $(1300/13.5)^2 \approx 9300$ beams are required, while 33 dishes requires 3000 beams [1]. With a potentially prohibitive number of beams, alternative approaches need to be considered, as discussed in [2]. In this paper, we examine a novel detector based on sums of covariance matrix elements. The detection performance and required computation of this are evaluated and compared to other approaches.

2 System Architecture

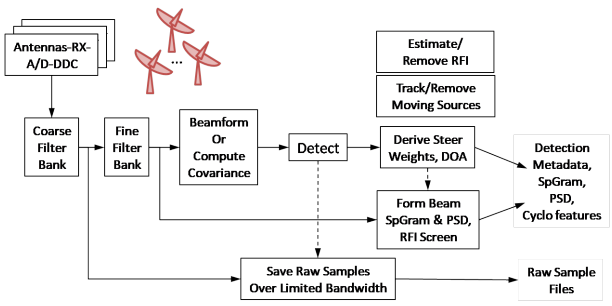

Figure 1. SETI Architecture

A notional system architecture is shown in Figure 1. We assume that frequency decomposition is done first, through use of multiple stages of polyphase filter banks (PFBs), down to the ultimate frequency resolution, on the order of a few Hz. The complex filter bank outputs are retained. Following this, detection is performed through beamforming and non-coherent averaging, or another technique. For each detection, the optimal steer weights are derived and the direction of arrival is estimated. A target beam is computed over a suitable bandwidth and spectrogram and power spectral density estimates are computed. Complex time-domain samples are collected over a limited bandwidth and duration to allow later analysis.

3 Signal Model

We assume that within a frequency bin, the signal is approximately zero frequency, and can be represented as a complex DC constant A and a phase factor $e^{j\Phi_i}$. Φ_i depends on the arrival direction and aperture offset from the array origin (phase center): $\Phi_i = \vec{k}_* \cdot \vec{x}_i = -(2\pi/\lambda)\vec{u}_* \cdot \vec{x}_i$ where $\vec{u}_*$ is the arrival unit vector pointing away from the earth. The noise consists of independent complex Gaussian variates whose real and imaginary parts are independent. We assume the signal has a random polarization common to all elements. The x and y polarization outputs are:

$$r_{x-i}(t) = Ae^{j\Phi_i} cos(\theta_{pol}) + n_{x-i}(t) \quad (1)$$
$$r_{y-i}(t) = Ae^{j\Phi_i} sin(\theta_{pol}) + n_{y-i}(t)$$

for $i = 1..N_{AP}$. In subsequent discussion, we use the terms "element", "aperture", and "dish" interchangeably, recognizing that an aperture array station might be used rather than a dish.

4 Detection Approaches

Four detection approaches were defined for evaluation, as described below. Detection is done on a bin-by-bin basis, with detectors running in parallel over all frequency bins. We assume all dish data are delay- and phase-aligned to the primary beam boresight direction so that subsequent "tied array" beams can be formed using simple complex weights for phase alignment.

The detection problem consists of choosing two hypotheses H0 and H1. Under H1, a signal is present with noise, while under H0, we are receiving noise alone. A detection statistic is computed at the end of an averaging interval $T_{avg} = N_{avg}/\Delta BW$, where ΔBW is the filterbank bandwidth, and compared to an appropriate threshold to decide between H0 and H1. The separation of the H0 and H1 statistics as a function of signal-to-noise ratio (SNR) at the element level determines the minimum detectable SNR for an allowable false alarm rate, and is a measure of sensitivity.

4.1 Beamform (BF)

This is a conventional beamformer, a coherent weighted sum over all elements, repeated for 2 polarizations and all pointing directions required to cover the primary FOV. Let ϕ_i^k be the steering phase for element i and beam k, which points in direction $\vec{u}_k$: $\phi_i^k = -(2\pi/\lambda)\vec{u}_k \cdot \vec{x}_i$. With $w_i^k = e^{-j\phi_i^k}$ (ignoring array shading), the beams are

$$b_{x-k}(t) = (1/N_{AP}) \sum_{i=0}^{N_{AP}-1} w_i^k \, r_{x-i}(t) \quad (2)$$
$$b_{y-k}(t) = (1/N_{AP}) \sum_{i=0}^{N_{AP}-1} w_i^k \, r_{y-i}(t)$$

Using an energy detector, the detection statistic for beam k is the mean of the magnitude square of each beam sample over the averaging interval and 2 polarizations:

$$DetBF_k = (1/N_{avg}) \sum_{t=0}^{N_{avg}-1} |b_{x-k}(t)|^2 + |b_{y-k}(t)|^2 \quad (3)$$

for $k = 1..N_{beam}$. The computation is simple, but repeats over a large number of beams. The total computation for each frequency bin (expressed as complex multiply-additions) scales as $CompBF = 2(N_{AP}+1)N_{avg}N_{beam}$.

4.2 Incoherent Beamform (IBF)

The incoherent beam is a sum of the squared magnitude of each element sample in both polarizations. As IBF(t) is already an energy quantity, the detection statistic is the mean over all time samples in the averaging interval.

$$IBF(t) = (1/N_{AP}) \sum_{i=0}^{N_{AP}-1} |r_{x-i}(t)|^2 + |r_{y-i}(t)|^2 \quad (4)$$
$$DetIBF = (1/N_{avg}) \sum_{t=0}^{N_{avg}-1} IBF(t)$$

Note that only one incoherent beam is required to cover the primary FOV, and the computation is least demanding, but this will be the least sensitive of all approaches. The compuation is given as $CompIBF = 2N_{AP}N_{avg}$.

4.3 Covariance Off-Diagonal Sum (CODS)

This is based on the sample covariance matrix, which is the average of the outer product of the element data vectors over all time samples. A single matrix is computed from the outer products of both polarizations. The ij element of the covariance matrix **R** is:

$$R_{ij} = (1/N_{avg}) \sum_{t=0}^{N_{avg}-1} r_{x-i}(t) r_{x-j}^*(t) + r_{y-i}(t) r_{y-j}^*(t) \quad (5)$$

Note that the DetIBF is the mean of the main diagonal of the covariance matrix. In contrast, the CODS detection statistic is the root-mean-square (RMS) sum of all elements above the main diagonal:

$$DetCODS = \sqrt{\frac{2}{N_{AP}(N_{AP}-1)} \sum_{i=0}^{N_{AP}-1} \sum_{j=i+1}^{N_{AP}-1} |R_{ij}|^2} \quad (6)$$

When implemented, the square root operation may be omitted. The main diagonal is excluded to avoid including products with correlated noise samples, which should improve the DetCODS statistical properties. A total of $N_{AP}(N_{AP}-1)/2$ entries of R are summed. With 2 polarizations, the computation is $CompCODS = N_{AP}(N_{AP}-1)(N_{avg}+1/2)$. Like the incoherent beam, only one sum is required to cover the primary FOV. We expect CODS to have sensitivity and computation in-between BF and IBF. A variant called Covariance Full Sum (CFS) is also defined for comparison, which performs an RMS sum of all elements in **R**.

4.4 Maximum Eigenvalue Detector

A detector from [3] based on the maximum eigenvalue λ_{MAX} of **R** is also included for comparison:

$$DetEig1 = \lambda_{MAX}/(Tr(\mathbf{R}) - \lambda_{MAX}) \quad (7)$$

Under H0, with independent unit-variance noise, the eigenvalues will each tend to unity. Under H1, the maximum eigenvalue will tend to $1+P_{sig}$, so DetEig1 will tend to $(1+P_{sig})/(N_{AP}-1) \propto (1+SNR)$. Two variants are considered: EIG1 computes all eigenvalues with $O({N_{AP}}^3)$ computation, and EIG2, which uses the power method at $O({N_{AP}}^2)$ computation, with $CompEig2 \approx 3\,CompCODS$.

5 Covariance-Based Detector Rationale

The rationale behind CODS and CFS is as follows. The value of the ij covariance matrix entry is:

$$R_{ij} = (1/N_{avg}) \sum_{t=0}^{N_{avg}-1} [r_{x-i}(t) r^*_{x-j}(t) + r_{y-i}(t) r^*_{y-j}(t)]$$
$$= (1/N_{avg}) \sum_{t=0}^{N_{avg}-1} [|A|^2 e^{j\Delta\Phi_{ij}} + n_{x-i}(t) n^*_{x-j}(t) + n_{y-i}(t) n^*_{y-j}(t) + cross\ terms] \quad (8)$$

The cross terms should average toward zero. The signal magnitude appears in each entry with a phase factor $\Delta\Phi_{ij} = \Phi_i - \Phi_j$, which should be consistent over the averaging interval. The noise terms in R_{ij} are products of Gaussian variates, which are approximately Gaussian if i≠j (off-diagonal) and chi-square if i=j. All noise terms of R_{ij} will reduce with averaging, but the off-diagonal noise terms will be zero mean. Once averaging R_{ij} is complete, and if A is large enough, the magnitude square operation in CODS or CFS should effectively remove the effect of the phase factor $\Delta\Phi_{ij}$, so $|R_{ij}|$ will consist of the signal magnitude squared $|A|^2$ plus a noise component. Beam steering or phase calibration is not required. CFS includes diagonal components i=j with non-zero-mean noise, while CODS does not.

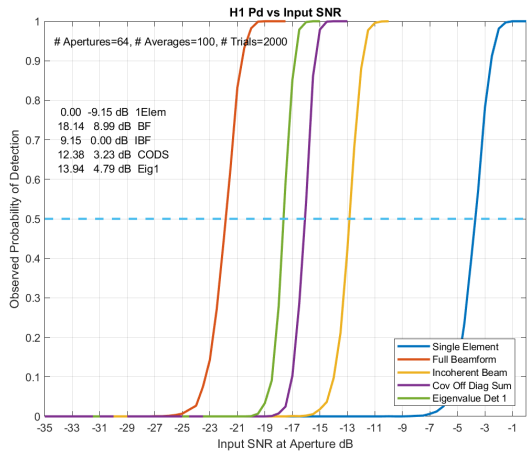

Figure 2. Detection Curves for Various Algorithms for $N_{AP} = 64$ and $N_{avg} = 100$

6 Simulation Description and Results

A simulation was conducted to examine the relative performance of the above detectors for various array sizes N_{AP} and averaging lengths N_{avg}. For a large number of trials, the phases Φ_i and weights $w_i = e^{-\Phi_i}$ were created and the amplitude A was swept over a wide range of element SNRs (for H1), or A was set to 0 (for H0). For simplicity, we did not model all possible arrival directions within the FOV but instead assumed that the element phases for each trial are random and uniformly distributed over $[0, 2\pi)$. We believe this should be a reasonable assumption over large baselines with a wide range of frequencies and arrival directions, but this can be verified with a higher-fidelity analysis and simulation. In order to avoid a potentially difficult analysis of specific H0 distributions, a detection threshold was set at $\gamma = \mu_0 + N_{std}\sigma_0$, where μ_0 and σ_0 were the observed H0 means and standard deviations, and N_{std} was set at $N_{std} = 6$, corresponding ideally to $P_{FA} = 10^{-9}$ for normal variables. This is a conservative choice. We don't expect the results for other thresholds to be markedly different.

A set of detection curves was created by evaluating histograms at various input SNRs and estimating the probability of detection Pd as a function of element SNR. An example for the various algorithms is shown in Figure 2 for for $N_{AP} = 64$ and $N_{avg} = 100$. Typical S-shaped curves are seen when plotting Pd vs SNR. The relative performance of the detectors can be assessed by examining the SNR offsets between the curves. We define the array gain AG_{dB} for a given N_{avg} as the difference in dB between the single element curve and the curve for each algorithm at Pd=50%.

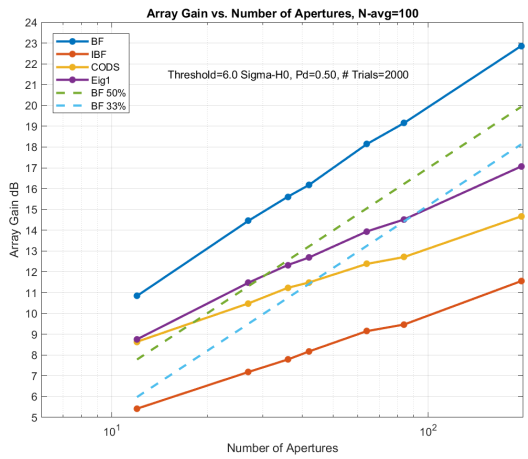

Figure 3. Relative Performance BF, IBF, EIG1 and CODS Algorithms vs. Number of Apertures N_{AP}

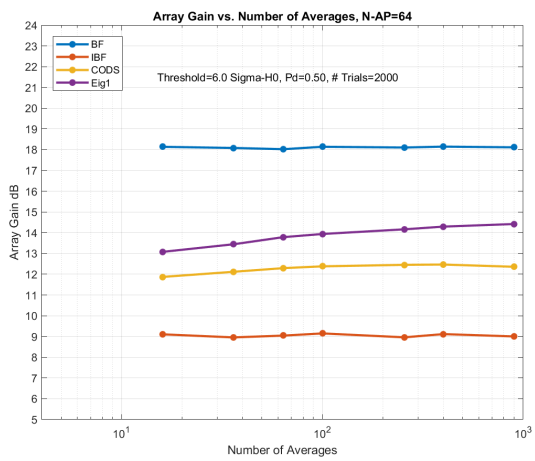

Figure 4. Relative Performance BF, IBF, EIG1 and CODS Algorithms vs. Number of Averages N_{avg}

With the reference Pd chosen, we can assess the relative merits of the detectors. We chose several array sizes corresponding to representative systems: N_{AP}=[12, 27, 36,

42, 64, 84, 197] corresponding to APERTIF, Jansky VLA, ASKAP, ATA-42, MeerKAT, MeerKAT Extension, and SKA1-Mid, respectively. The measured array gains are plotted for BF, CODS, EIG1 and IBF versus the number of apertures (Figure 3) and versus the number of averages (Figure 4). The BF case assumes 100% of elements are used, but Figure 3 also includes theoretical curves for BF using subarrays with 50% and 33% elements (dashed lines). Table 1 tabulates the array gain relative to IBF versus N_{AP}.

	N_{AP}						
	12	27	36	42	64	84	197
BF 100%	5.4	7.3	7.8	8.0	9.0	9.7	11.3
BF 50%	2.4	4.1	4.8	5.1	5.9	6.8	8.4
BF 33%	0.6	2.3	3.0	3.2	4.1	5.0	6.6
Eig1	3.3	4.3	4.5	4.5	4.8	5.1	5.5
CODS	3.2	3.3	3.4	3.3	3.2	3.2	3.1
IBF	0.0	0.0	0.0	0.0	0.0	0.0	0.0
1Elem	-5.4	-7.2	-7.8	-8.2	-9.1	-9.5	-11.6

Table 1. Estimated Array Gain over IBF (dB), N_{avg}=100 vs. Number of Apertures N_{AP}

7 Discussion

Some notes and observations:

- BF and IBF trend almost exactly to the classical expressions AG_{dB}=10log(N_{AP}) and 5log(N_{AP}) respectively. BF is the most sensitive and IBF the least.
- CODS offers 3.2 dB better performance than IBF, with AG_{dB} = 5log(N_{AP}) + 3.2, but is 2-8 dB worse than full BF, depending on array size.
- EIG1 has $AG_{dB} \approx$ 6.4log(N_{AP}) + 2.3, 0-2 dB above CODS. CODS is comparable to EIG1 for N_{AP}=12. EIG1 is still 2-6 dB less sensitive than BF.
- The power method EIG2 algorithm is within .15 dB of EIG1 for $N_{avg} \geq 64$, at ∼3x the computation of CODS.
- The relative performance between the various detectors is insensitive to the number of averages N_{avg}, except EIG1 which increases slightly with N_{avg}.
- Taking into account lower AG due to fewer elements in the array core and scalloping and calibration losses, CODS and EIG1 may be competitive with BF in practice. The BF 33% line may actually be what is achieved with 50% core elements.
- Given that detection rate scales as $AG^{3/2}$ [2], we would expect relative rates of 1.0 (IBF), 3.1 (CODS), 5.2 (EIG1) and 22 (100% BF over full FOV) for N_{avg}=100 and N_{AP}=64, but huge differences in compute costs.

In the simulations, the Covariance Full Sum (CFS) variant of CODS consistently has 1 dB less gain than CODS, a result of correlated noise in the diagonal elements of **R**. CFS is clearly inferior. A CODS variant called "Covariance Off-Diagonal Absolute Sum" (CODAS) was also examined, which calculates mean($|R_{ij}|$) rather than RMS($|R_{ij}|$) for off-diagonal elements. CODAS has nearly identical performance (within .1-.4 dB), so this could be used in place of CODS.

One significant benefit of CODS and EIG1/EIG2 over IBF may be in radio-frequency interference (RFI) rejection. Interferometric arrays are potentially less sensitive to RFI because of the path diversity from RFI sources to individual apertures. This will partly decorrelate the RFI cross-products (visibilities). Therefore one may expect CODS and EIG1/EIG2 to be less susceptible to RFI than IBF. When RFI forces a detection, the covariance matrix is available to allow separation of the interferer from the desired signal and noise. Once isolated, it may be possible to recognize the interference and reject it. Features to recognize RFI might include coherence across the array (or lack of it), direction of arrival, low elevation angle, angular motion, or cyclostationary properties.

One caveat about the covariance methods: **R** must be coherently summed over the full observation interval for both EIG1 and CODS to attain the gains reported above. If DetCODS or DetEIG1 from subintervals are combined to form a longer interval, the net gain over IBF decreases to only ∼1 dB. If searching for chirp signals spanning many frequency bins over T_{avg}, we need to combine **R**, not DetCODS or DetEIG1, over the appropriate bins and subintervals.

8 Conclusions and Further Steps

A novel detector was described and evaluated for peformance against other candidate algorithms. The CODS detector should offer 3 dB more sensitivity over incoherent beamforming at a considerable cost reduction compared to Eigenvalue detectors or full beamforming. The utility of CODS is not limited to narrowband signals, but could be used for rapid detection of pulsars and fast radio bursts. Clearly the next steps involve developing higher-fidelity simulations, and examining real data sets.

9 Acknowledgements

Breakthrough Listen is managed by the Breakthrough Initiatives, sponsored by the Breakthrough Prize Foundation.

References

[1] Justin Jonas, "The MeerKAT Radio Telescope," *Proceedings of Science (MeerKAT2016)*, 2018, doi: 10.22323/1.277.0001.

[2] K.M. Houston, A.P.V. Siemion, and S. Croft , "Strategies for Maximizing Detection Rate in Radio SETI", in preparation.

[3] S. W. Ellingson, "Detection of Tones and Pulses Using a Large, Uncalibrated Array," IEEE Antennas and Propagation Society International Symposium. Columbus, OH, 2003, pp. 196-199 vol.4.